

# Determination of the three-dimensional lattice mismatch in quaternary III-V liquid phase epitaxial layers using simultaneous Bragg diffraction of x rays

Shih-Lin Chang

Instituto de Física "Gleb Wataghin," Universidade Estadual de Campinas, 13100 Campinas, S.P. Brasil

(Received 16 June 1980; accepted for publication 15 August 1980)

Because multiple simultaneous reflection of x rays is very sensitive to lattice deformation, the six-beam, (000) (006) ( $\bar{2}\bar{2}4$ ) ( $\bar{2}\bar{2}2$ ) ( $2\bar{2}4$ ) ( $2\bar{2}2$ ) multiple reflection was used to record simultaneously the information about the lattice mismatch of [001] InGaAsP materials using a divergent x-ray source. The lattice mismatches in directions parallel and perpendicular to [001], determined from a single divergent-beam photograph, increase as the As concentration in liquid composition  $X'_{As}$  increases. The procedure was used without difficulty for  $X'_{Ga}$  as low as 0.0007 and  $X'_{As}$  in the range 0.006–0.01.

PACS numbers: 68.55. + b, 61.10.Fr

Uneven liquid phase epitaxial (LPE) layer surfaces usually cause unfavorable increases in threshold current density and optical scattering loss of double-heterojunction (DH) lasers, and efforts have been made<sup>1-4</sup> to improve surface morphology. Recently Prince *et al.*<sup>5</sup> reported that the improvements of the surface morphology of the InGaAsP DH laser system by adding small amounts of Ga and As in the layers confining the active region made possible the fabrication of good-quality wafers with low threshold current density and high yield. In the course of crystal growth of these small-x and -y confining quaternary layers, the divergent-beam method<sup>6</sup> was employed to detect lattice mismatch. As is known, a single x-ray measurement from a single reflection can only give information of lattice mismatch in one direction. The determination of  $\Delta a_{\perp}$  and  $\Delta a_{\parallel}$  for [001] InGaAsP/InP can be obtained from at least three x-ray measurements.<sup>7-9</sup>  $\Delta a_{\perp}$  and  $\Delta a_{\parallel}$  are equal to  $a_{\perp} - a_s$  and  $a_{\parallel} - a_s$ , where  $a_s$ ,  $a_{\perp}$ , and  $a_{\parallel}$  are the lattice constants for the substrate and for the epi-layer in the directions normal and parallel to the interfacial plane. In this letter, we report that by using multiple reflection we are able to obtain three-dimensional information about the lattice mismatch between the epitax-

ial layer and substrate from a single divergent-beam photograph by utilizing multiple diffraction effects.

For a cubic [001] InP crystal, six-beam multiple reflection, (000) (006) ( $\bar{2}\bar{2}4$ ) ( $\bar{2}\bar{2}2$ ) ( $2\bar{2}4$ ) ( $2\bar{2}2$ ), occurs when the crystal is first placed in position for (006) reflection and is then rotated around the normal to (006) to bring [1 $\bar{1}$ 0] to the plane of incidence (Fig. 1). These six reciprocal lattice points remain on the Ewald sphere and diffract simultaneously. Interactions among them, within the crystal, give rise to variations in the (006) reflected intensity.<sup>10</sup> In Fig. 1,  $\theta_B$  and  $\phi$  are the Bragg angle of the (006) reflection and the azimuthal angle of rotation, respectively, and  $\beta$  is the angle between the plane of incidence and the plane containing the six reciprocal lattice points. Owing to small differences between  $a_{\perp}$  and  $a_{\parallel}$ , InGaAsP quaternary-compound layers have tetragonal unit cells.<sup>8</sup> The corresponding six reciprocal lattice points can then no longer be brought simultaneously onto the surface of the Ewald sphere. Instead, only four points, either [(000) (006) ( $\bar{2}\bar{2}4$ ) ( $\bar{2}\bar{2}2$ )] (set 1) or [(000) (006) ( $2\bar{2}4$ ) ( $2\bar{2}2$ )] (set 2) can enter or leave the Ewald sphere together. The six-beam multiple reflection for a cubic system is then decomposed into two four-beam cases for a tetragonal. One four-beam set, say set 1, enters just after the other, set 2, leaves the Ewald sphere. The ordering of the sequence is reversed after  $\beta = 90^\circ$ , when set 1 leaves just after set 2 enters the Ewald sphere. Therefore the angle  $\beta$  has the same value but a different sign for the two cases of four-beam reflection. The corre-

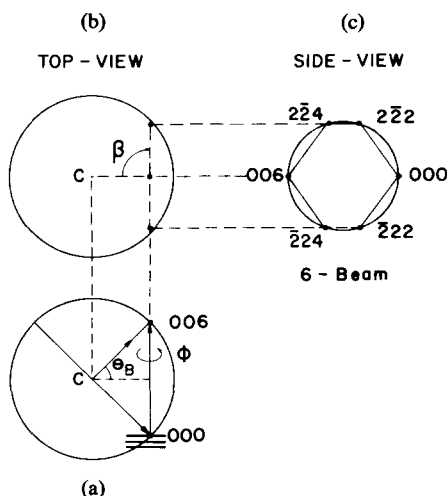


FIG. 1. Geometry of six-beam multiple reflection of x rays in reciprocal space: (a) in plane of incidence, (b) top view of (a), (c) side view of (b).

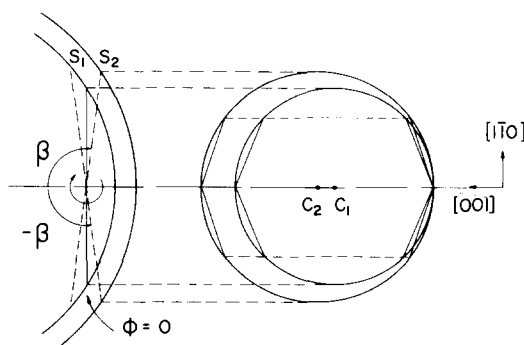


FIG. 2. Top and side views of Fig. 1(a) for a cubic system and a tetragonal system with  $\Delta a_{\perp} \neq 0$  and  $\Delta a_{\parallel} = 0$ .  $C_1$  and  $S_1$  are the center and circle for cubic and  $C_2$  and  $S_2$  for tetragonal.

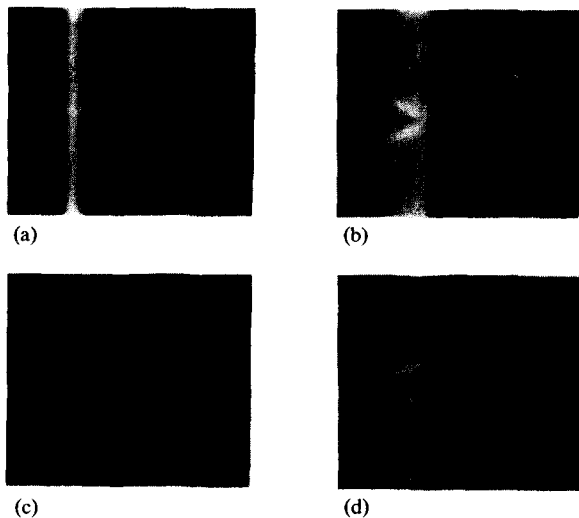


FIG. 3. (006) reflection images in the vicinities of (a) the six-beam case for InP and of the four-beam cases for InGaAsP with  $X'_{As}$  equal to (b) 0.010 5, (c) 0.009 9, and (d) 0.009 1, where  $X'_{Ga} = 0.000\ 69$ . Cu  $K\alpha_1$  lines are on the left of the Cu  $K\alpha_2$  lines.

sponding azimuths  $\phi$  are then equal to  $\beta - 90^\circ$  and  $90^\circ + \beta$ , respectively. This is illustrated in Fig. 2 for  $\Delta a_{||} = 0$ .

According to Cole *et al.*,<sup>11</sup>  $\beta$  for a tetragonal system can be calculated as

$$\cos\beta = \left( \frac{h^2 + k^2}{a_{||}^2} + \frac{l^2 - lL}{a_1^2} \right) \times 2 \left( \frac{h^2 + k^2}{a_{||}^2} \right)^{1/2} \left( \frac{1}{\lambda^2} - \frac{L^2}{4a_1^2} \right)^{1/2} \quad (1)$$

if the rotation axis is  $[00L]$  and the additional reflection is  $(hkl)$ .  $\lambda$  is the wavelength of the x ray used. For InP ( $a_{||} = a_1$ ) and Cu  $K\alpha_1$  radiation,  $\beta$  is  $90^\circ$ . For the quaternary layer, the deviation  $\Delta\beta$  from  $90^\circ$  can be obtained as

$$\Delta\beta = [(h^2 + k^2)\Delta a_{||} + (l^2 - lL)\Delta a_1] \times a_s (h^2 + k^2)^{1/2} \left( \frac{1}{\lambda} - \frac{L^2}{4a_s^2} \right), \quad (2)$$

where  $a_s$  is  $5.8696\ \text{\AA}$  for InP. For these particular four-beam cases,

$$\Delta\beta = 0.205(\Delta a_{||} - \Delta a_1), \quad (3)$$

where  $\Delta a_1$  and  $\Delta\beta$  can be determined by  $\Delta a_1/a_s$ ,

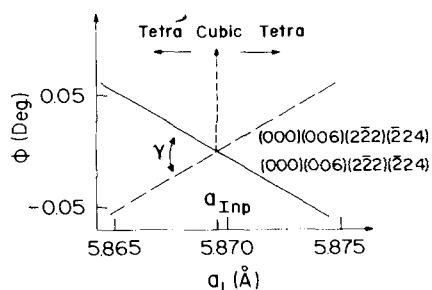


FIG. 4. Calculated azimuthal positions  $\phi$  for two four-beam multiple reflections against  $a_1$  ( $\Delta a_{||} = 0$ ).

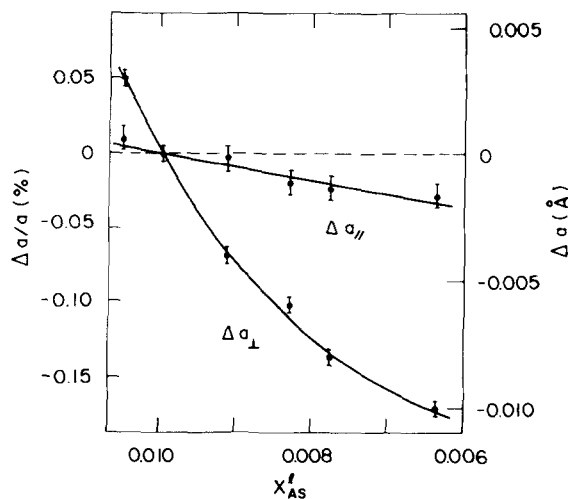


FIG. 5. Measured  $\Delta a_{||}$  and  $a_1$  for various  $X'_{As}$ , where  $X'_{Ga} \sim 0.000\ 69$ .

$= -\cot\theta_B \Delta\theta$  and from the angular separation between the two four-beam reflection lines.  $\Delta a_{||}$  is then determined.

Experimental investigations were carried out using the divergent-beam setup previously described.<sup>6</sup> The  $5^\circ$  beam divergence simplifies the alignment problem and makes possible the recording in one photograph of regions in reciprocal space included within a  $5^\circ$  azimuthal rotation. Films were placed 150 cm from the sample to detect the (006) reflection. The thicknesses of the InP substrate and the InGaAsP layer were about 500 and  $5\ \mu\text{m}$ , respectively. In Fig. 3, the images are shown of the (006) reflection in the vicinities of the six-beam case for InP and of the four-beam cases for InGaAsP with various As concentrations in the liquid composition  $X'_{As}$ . Comparisons can be made with the calculated image, with  $\Delta a_{||} = 0$ , given in Fig. 4. Since the horizontal and vertical axes represent respectively  $\Delta(2\theta)$  and  $\Delta(2\beta)$ , the slopes of the four-beam reflection lines can be determined by

$$\tan\frac{1}{2}\gamma = \Delta\beta / 2\Delta\theta, \quad (4)$$

where  $\gamma$  is the angle between the two four-beam reflection lines. From Eqs. (3) and (4) it is clear that the slope is a function of  $\Delta a_{||}$  and  $\Delta a_1$ . It is constant if  $\Delta a_{||}$  is linearly proportional to  $\Delta a_1$ .

It is known that  $a_1$  varies continuously along the interface normal. A broad reflection band is common for the quaternary layer.  $\Delta a_1$  and  $\Delta a_{||}$  were determined by measuring  $\Delta\theta$  and  $\Delta\beta$  at the middle of the reflection band from the enlarged ( $\times 10$ ) images of the original divergent-beam photographs. In Fig. 5, the measured  $\Delta a_1$  and  $\Delta a_{||}$  are given as functions of  $X'_{As}$  with  $X'_{Ga} \cong 0.000\ 69$ . They resemble the curves obtained by Oe *et al.*<sup>8</sup> for  $X'_{As}$  and  $X'_{Ga}$  one order of magnitude higher. The errors indicated here were estimated from the widths of the reflection lines.

The above provides a method of determining  $\Delta a_{||}$  and  $\Delta a_1$  from a single divergent-beam x-ray photograph using multiple reflection. Although the test of this method was made for confining quaternary layers with small  $x$  and  $y$ , it is applicable to any  $[001]$  InGaAsP quaternary layer with different  $x$  and  $y$ . However, for  $[111]$  oriented quaternary mate-

rials, one should look for other multiple reflection sets for such investigations.

Financial support from TELEBRÁS, CNPq, and BID is gratefully acknowledged.

<sup>1</sup>J. C. Dymont, F. R. Nash, C. J. Hwang, G. A. Rozgonyi, R. L. Hartman, H. M. Marcos, and S. E. Haszko, *Appl. Phys. Lett.* **24**, 481 (1974).

<sup>2</sup>G. H. B. Thompson, P. A. Kirkby, and J. E. A. Whiteaway, *IEEE J. Quantum Electron.* **QE-11**, 481 (1975).

<sup>3</sup>F. R. Nash, W. R. Wagen, and R. L. Brown, *J. Appl. Phys.* **47**, 3992 (1976).

<sup>4</sup>T. Fukui and T. Kobayashi, *Jpn. J. Appl. Phys.* **18**, 2307 (1979).

<sup>5</sup>F. C. Prince, N. B. Patel, and D. J. Bull (unpublished).

<sup>6</sup>S.-L. Chang, N. B. Patel, Y. Nannichi, and F. C. Prince, *J. Appl. Phys.* **50**, 2975 (1979).

<sup>7</sup>K. Ishida, J. Matsui, T. Kamejima, and I. Sakuma, *Phys. Status Solidi (a)* **31**, 255 (1975).

<sup>8</sup>K. Oe, Y. Shinoda, and K. Sugiyama, *Appl. Phys. Lett.* **33**, 962 (1978).

<sup>9</sup>J. Matsui, K. Onabe, T. Kamejima, and I. Hayashi, *J. Electrochem. Soc.* **126**, 664 (1979).

<sup>10</sup>R. M. Moon and C. G. Shul, *Acta Crystallogr.* **17**, 805 (1964).

<sup>11</sup>H. Cole, F. Chambers, and H. Dunn, *Acta Crystallogr.* **15**, 138 (1962).

## High-temperature scanning cw laser-induced diffusion of arsenic and phosphorus in silicon

S. Matsumoto<sup>a)</sup> and J. F. Gibbons

*Stanford Electronics Laboratories, Stanford, California 94305*

V. Deline and C. A. Evans, Jr.

*Charles Evans and Associates, San Mateo, California 94400*

(Received 30 June 1980; accepted for publication 23 August 1980)

The diffusion of arsenic and phosphorus in silicon at temperatures near the melting point has been investigated by using a scanned cw laser. The intrinsic diffusion coefficients of arsenic and phosphorus obtained in this work agree well with the extrapolated values of intrinsic diffusion coefficients reported by others. Diffusion coefficients of arsenic under extrinsic conditions at temperatures over 1200 °C are found to depend linearly on the electron concentration. The validity of the analytical model for solid-phase reaction expressed in terms of an effective temperature and an effective time for the laser heat source is shown.

PACS numbers: 66.30.Jt

It has been shown that both pulsed and cw lasers can be used to recrystallize damage produced during ion implantation and to activate implanted dopants completely.<sup>1-4</sup> In pulsed laser annealing, a liquid layer is thought to form during the annealing process and implanted dopants are then rapidly redistributed through the liquid layer. The redistribution of dopants has been explained using a model based on the diffusion of dopants in liquid silicon.<sup>5-7</sup> On the other hand, the scanning cw laser can produce solid-phase recrystallization of the implanted layers, which yields no diffusion of implanted dopants during the annealing cycle. In this case, the dwell time of a single scan is on the order of 1 msec under typical scanning conditions, which is too short to cause the significant diffusion of implanted dopants.

In this letter, the diffusion of implanted arsenic and phosphorus in silicon has been investigated using multiple scans of a cw laser, which increases the equivalent dwell time substantially. By using roughly 1000 scan frames we obtain a total diffusion time on the order of 1 sec, which is then sufficient to produce easily measurable diffusion at temperatures in the vicinity of the melting point.

The theoretical basis for the experiments to be described here is contained in the analytical model for solid-phase reactions induced by scanning cw laser developed by Gold and Gibbons.<sup>8</sup> These authors show that the effect of laser irradiation can be interpreted in terms of an "effective temperature"  $T_{\text{eff}}$  and an "effective time"  $t_{\text{eff}}$  even though the temperature in the laser annealing process is actually a function of time. This model can be applied to the laser-induced diffusion studies of this work by using the expression

$$x^2 = D_0 t_{\text{eff}} \exp(-E_a/kT_{\text{eff}}), \quad (1)$$

where  $x$  is the diffusion length,  $D_0$  is the preexponential factor, and  $E_a$  is the activation energy of impurity for diffusion.

For the case of multiple overlapping scans (i.e., multiple scan frames),  $T_{\text{eff}}$  and  $t_{\text{eff}}$  are given by<sup>8</sup>

$$T_{\text{eff}} = T_{\text{max}} = T_k + (T_0 - T_k) \exp(P/2\sqrt{\pi} w A), \quad (2)$$

$$t_{\text{eff}} = t_{\text{tot}} (\pi r_{\text{eff}}^2) / A_{\text{tot}}, \quad (3)$$

where  $T_{\text{max}}$  is the maximum temperature of the surface,  $T_0$  is the substrate backside temperature,  $P$  is the laser power,  $w$  is the Gaussian beam radius,  $T_k$  and  $A$  are constants equal to 99 K and 299 W/cm, respectively, for silicon,  $t_{\text{tot}}$  is the total scan time,  $A_{\text{tot}}$  is the total scan area, and  $r_{\text{eff}}$  is the effective

<sup>a)</sup>On leave from Keio University, Japan.